

Heat and mass transport in icy worlds (melting/freezing, porous flow)

Gaël Choblet

Laboratoire de planétologie et géodynamique, CNRS-Université de Nantes

The Solar System:



Moons with colored frames are not to scale.

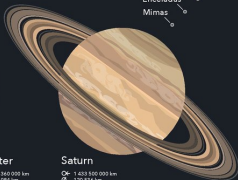
☉ = distance of the planet to the sun
⊙ = average- or equatorial diameter

Vesta
Juno
Asteroid belt
Ceres
Pallas



Jupiter

☉ 778 360 000 km
⊙ 142 984 km
79 moons (in total)



Saturn

☉ 1 433 500 000 km
⊙ 120 536 km
82 moons (in total)

ring system of Saturn: not in scale

Hyperion
Titan
Rhea
Dione
Tethys
Enceladus
Mimas



Uranus

☉ 2 872 000 000 km
⊙ 51 118 km
27 moons in total



Neptune

☉ 4 498 400 000 km
⊙ 49 528 km
14 moons in total

Scale (disproportion)
20 000 40 000 60 000 km

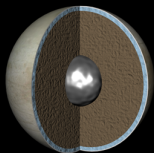
The major objects in the belt
not in scale



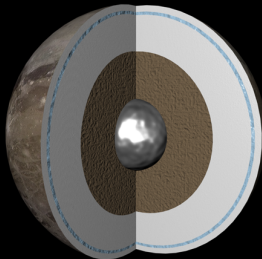
Scale representation of the distances of the objects to the sun
Scale: 1 AU (149.6 Mill. km)

Eris
Makemake
Kuiper belt
Pluto
Charon
Haumea

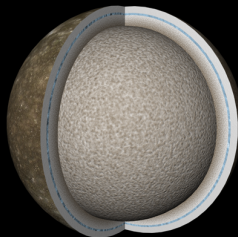
The major dwarf
planets including the
biggest moon of Pluto
in scale.



Europa

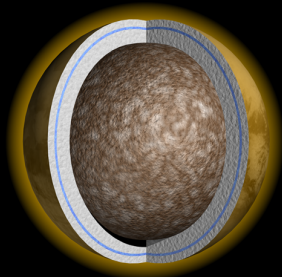


Ganymede

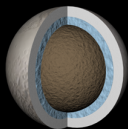


Callisto

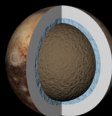
- Key**
- ice
 - water
 - rock
 - metal



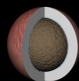
Titan



Eris



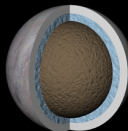
Pluto



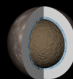
Sedna



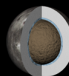
Enceladus



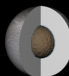
Triton



Titania



Oberon



Rhea

Outlook

-) solid state convection in planetary layers
-) balance laws and a boundary condition
-) solid-state convection with a phase change at the boundary
- v) porous convection in the rocky core of Enceladus

Solid-state convection in planetary interiors

Conservation of mass:

$$\frac{\partial \rho}{\partial t} + \nabla \cdot \rho \mathbf{V} = 0$$

Solid-state convection in planetary interiors

Conservation of mass:

$$\nabla \cdot \mathbf{V} = 0$$

- ▶ incompressible fluids (not really true for large bodies),
or at least anelastic approximation,

Solid-state convection in planetary interiors

Conservation of momentum:

$$\frac{1}{\text{Pr}} \left[\frac{\partial \mathbf{V}}{\partial t} + \mathbf{V} \cdot \nabla \mathbf{V} \right] = -\nabla p^* + \nabla \cdot \eta (\nabla \mathbf{V} + \nabla \mathbf{V}^t) + \text{Ra} T \gamma_z$$

- ▶ p^* : non-hydrostatic pressure,
- ▶ infinite Prandtl number fluids (diffusion of momentum way faster than diffusion of heat): non-linear inertial terms disappear
⇒ no mechanical turbulence, strongly simplifies dynamics!
- ▶ rheology is very complex... (temperature dependent, grain-size dependent and affects grain size, non-Newtonian)
⇒ strongly complexifies dynamics!
⇒ spectral approaches (spherical harmonics) lose elegance, grid-based methods used in practice.

Solid-state convection in planetary interiors

Conservation of momentum:

$$0 = -\nabla p^* + \nabla \cdot \eta (\nabla \mathbf{V} + \nabla \mathbf{V}^t) + \text{Ra} T \gamma_z$$

- ▶ p^* : non-hydrostatic pressure,
- ▶ infinite Prandtl number fluids (diffusion of momentum way faster than diffusion of heat): non-linear inertial terms disappear
⇒ no mechanical turbulence, strongly simplifies dynamics!
- ▶ rheology is very complex... (temperature dependent, grain-size dependent and affects grain size, non-Newtonian)
⇒ strongly complexifies dynamics!
⇒ spectral approaches (spherical harmonics) lose elegance, grid-based methods used in practice.

Solid-state convection in planetary interiors

Conservation of momentum:

$$0 = -\nabla p^* + \nabla \cdot \eta (\nabla \mathbf{V} + \nabla \mathbf{V}^t) + \text{Ra} T \gamma_z$$

- ▶ p^* : non-hydrostatic pressure,
- ▶ infinite Prandtl number fluids (diffusion of momentum way faster than diffusion of heat): non-linear inertial terms disappear
⇒ no mechanical turbulence, strongly simplifies dynamics!
- ▶ rheology is very complex. . . (temperature dependent, grain-size dependent and affects grain size, non-Newtonian)
⇒ strongly complexifies dynamics!
⇒ spectral approaches (spherical harmonics) lose elegance, grid-based methods used in practice.

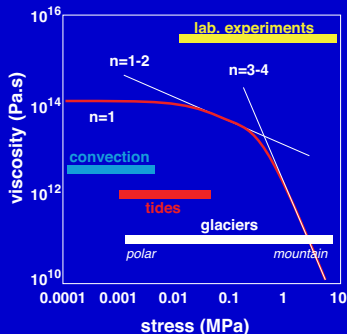
Rheology: exemple of ice I

Viscosity

$$\frac{1}{\eta} = \frac{1}{\eta_{diff}} + \frac{1}{\eta_{disl}} + \frac{1}{\eta_{gbs} + \eta_{bs}}$$

with

$$\eta_{\bullet} = \frac{d_{\bullet}^m}{A_{\bullet} \sigma_{II}^{n_{\bullet}-1}} \exp\left(\frac{E_{\bullet} + pV_{\bullet}}{RT}\right)$$

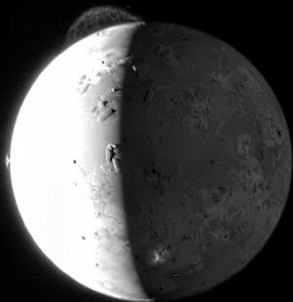


Solid-state convection in planetary interiors

Conservation of energy:

$$\frac{\partial T}{\partial t} + \mathbf{V} \cdot \nabla T = \nabla^2 T + \tilde{h}$$

- ▶ heat transfer as the sole control of time evolution,
- ▶ \tilde{h} : heat sources/sinks possibly involving secular cooling/heating, decay of long-lived radio-isotopes (mostly in rocks), tidal heating,
- ▶ typically solved with a *minmod* limiter approach for the advective flux.



Convection with an open boundary

Heat pipe mechanism, Io (O'Reilly and Davies, 1981)

First Voyager observations paradoxical:

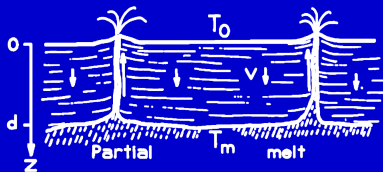


Fig. 1. Model of Ionian lithosphere. Magma at temperature T_m rises through vents and spreads across surface, cooling to surface temperature T_0 . Weight of flows depresses lithosphere at subsidence velocity v , which equals resurfacing rate.

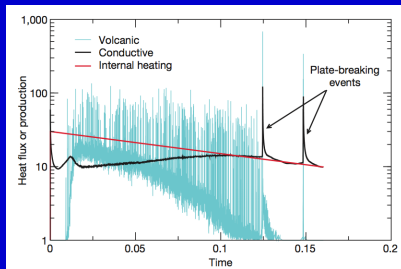
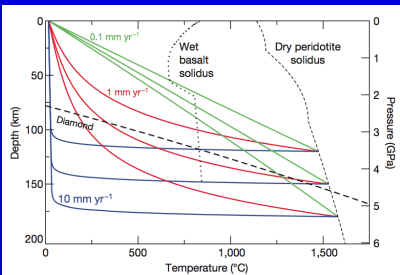
- ▶ very large surface heat flux (2 ± 1 W.m^{-2} at the time, 2.4 ± 0.9 W.m^{-2} today) \Rightarrow thin conducting lithosphere (few kms),
- ▶ however large reliefs (*"apparently of silicate composition"*) in excess of 10 kms were observed...

Among other possibilities (dynamic support, low density roots), the authors favor the possibility of very efficient magmatic heat transport allowing a much thicker conductive lithosphere.

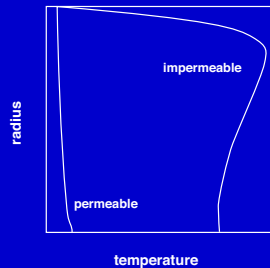
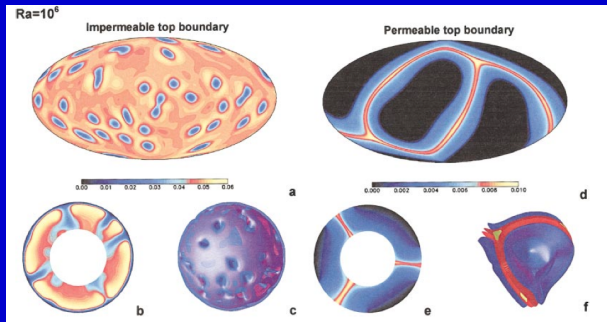
Heat pipe mechanism, early Earth (Moore and Webb, 2013)

On Earth, the > 3.2 Gyr old geological record often interpreted in terms of *proto plate-tectonics* or *vertical tectonics*. However, heat-pipe cooling could be a more appealing mechanism:

- ▶ Greenstone belts (Pilbara, Australia ; Barberton, South Africa) globally devoid of deformation (except for diapirs), longlasting rapid volcanic resurfacing, downward advection consistent with petrology of TTG plutons.
- ▶ Jack Hills zircons hosting diamonds with surface signature exhumed again by the ascent of TTG plutons (intersection of wet basalt and heat pipe geotherms in the diamonds stability field),
- ▶ abrupt cessation of heat-pipe volcanism coincides with onset of plate tectonics in numerical models.

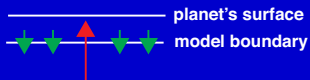


Heat pipe mechanism, Io (Monnereau and Dubuffet, 2002)



Boundary conditions

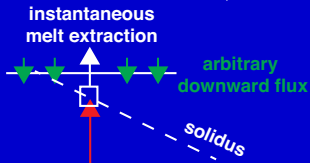
Monnereau and Dubuffet, 2002:



To mimick the heat pipe effect, a permeable boundary is introduced at the surface of the model (i.e. slightly below the actual planetary surface):

- ▶ $\tau_{rr} = 0, V_h = 0,$
- ▶ $\partial T / \partial r = 0,$ with an upwind-like scheme:
(cold) outside T prescribed when $V_r > 0,$
(hot) inside T prescribed when $V_r < 0.$

Moore and Webb, 2013:

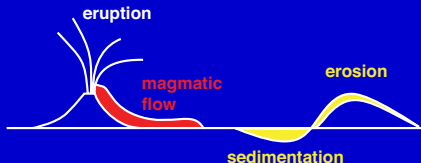


To mimick the heat pipe effect, downward advection with velocity v is prescribed:

- ▶ $\partial^2 T / \partial z^2 = v \partial T / \partial z - \tilde{h},$
- ▶ melt is extracted instantaneously.

Convection in hot planets (Ricard et al., 2014)

A more general framework can be introduced with a free surface condition subjected to **erosion/sedimentation** as well as **magmatic cooling**:

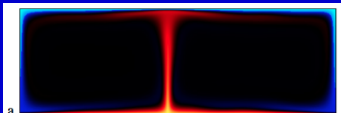


- ▶ free-surface formulation with a diffusing topography h :
 $\sigma_{zz} = -\rho gh$, $\tau_{xz} = \tau_{yz} = 0$, Eulerian vertical velocity $v_h = \nabla \cdot (D\nabla h)$,
- ▶ diffusivity $D = D_e + D_m$,
 $D_e = 10^{-6} - 10^{-3} \text{ m}^2 \cdot \text{s}^{-1}$ (empirically determined),
 $D_m = 1 - 10^9 \text{ m}^2 \cdot \text{s}^{-1}$ (depending on magma viscosity),
- ▶ a secondary Rayleigh number is introduced for topography: $R = \rho g H^3 / \eta D$ (topographic resistance),
- ▶ this formulation continuously spans surface conditions ranging from a closed ($R \rightarrow \infty$) to an open ($R \rightarrow 0$) system.

Convection in hot planets (Ricard et al., 2014)

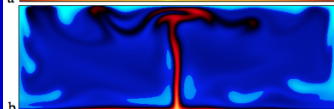
$$Ra = 10^6$$

$$R = 10^5$$



a

$$R = 10^4$$



b

$$R = 10^3$$

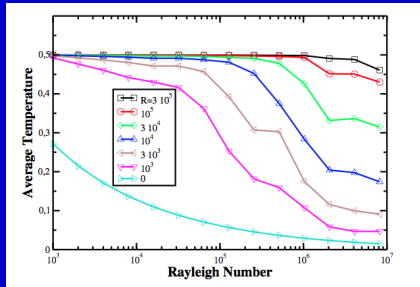


c

$$R = 0$$



d



- ▶ resistance R controls the level of surface opening,
- ▶ a threshold value of $\sim Ra/10 - Ra/100$ is identified.

Interface subjected to advection and phase change (Deguen, Alboussière)

- continuity of normal stress

(convective stresses equal weight of topography h):

$$-p + 2\eta \frac{\partial v_r}{\partial r} = \Delta \rho g h$$

- velocity of phase change V_r equal to radial velocity in solid v_r
(if h varies slowly):

$$V_r = -\frac{h}{\tau_\phi} - A \left(\frac{q_T^s}{\rho_l c_{p,l}} - q_\chi^s \right) \simeq v_r$$

where τ_ϕ is a characteristic time scale for the phase change
(involving heat transfer in the liquid) and q_\bullet^s are fluxes (of heat and
solute) on the solid side.

Interface subjected to advection and phase change (Deguen, Alboussière)

both expressions combined lead to (dimensionless equation):

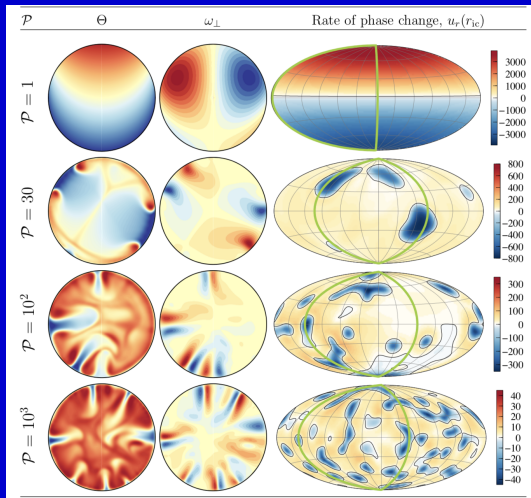
$$-p + 2 \frac{\partial v_r}{\partial r} = \mathcal{P} \left[v_r - \frac{1}{S} \left(q_T^s + \frac{\kappa_\chi \Delta c}{\kappa_T \Delta T} q_\chi^s \right) \right]$$

where

$$\mathcal{P} = \frac{\Delta \rho g R \tau_\phi}{\eta}$$

is the ratio between characteristic time scale for phase change (τ_ϕ) and the viscous time scale, indicative of the amount of permeability.

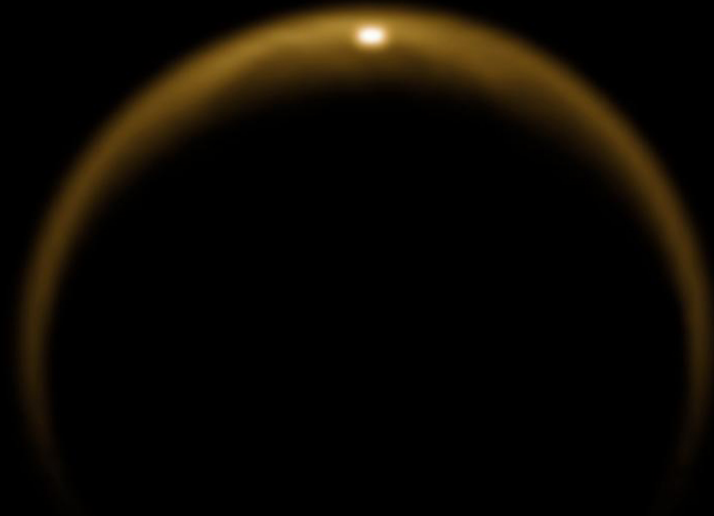
Translation of Earth's inner core



- ▶ for large viscosities (low \mathcal{P}) values, convective translation of the inner core is the most probable outcome, explaining paradoxical stratified layer observed by seismology at the inner-core boundary.

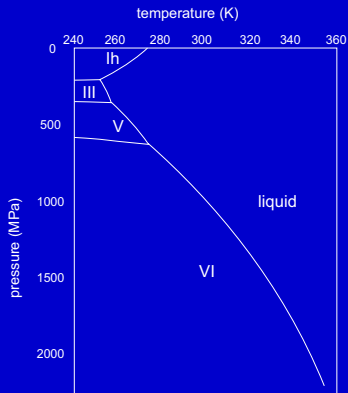
Main effects of a permeable boundary on thermal convection:

- ▶ the onset of convection possibly shifted to lower thresholds,
- ▶ convection pattern strongly affected (longer wavelengths promoted),
- ▶ heat transfer enhanced and cool layers with hot pipes.



Heat and mass transfer in high-pressure ice mantles

Water phase diagram (*Choukroun and Grasset, 2007*)



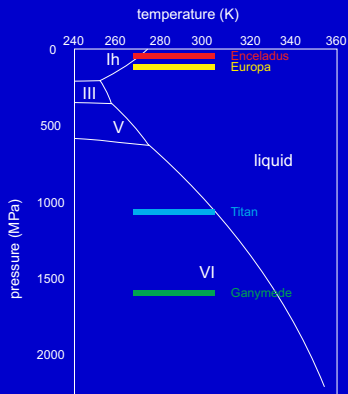
ice polymorphs present in Solar System's moons:

- ▶ hexagonal ice Ih
- ▶ high-pressure ices: II, III, V, VI

Water phase diagram

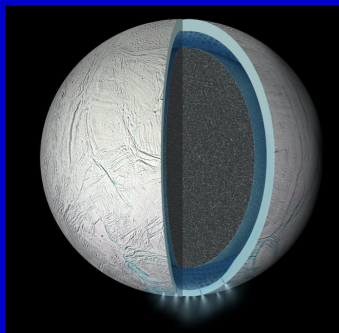
depth of water/rock contact:

moon	$R_s - R_{w/r}$ (km)	g (m/s ²)	$P_{w/r}$ (MPa)
Enceladus	50	0.11	10
Europa	100	1.31	130
Titan	550	1.35	1100
Ganymede	800	1.43	1600



if ocean present beneath an icy crust, isentropic temperature profiles within ocean imply

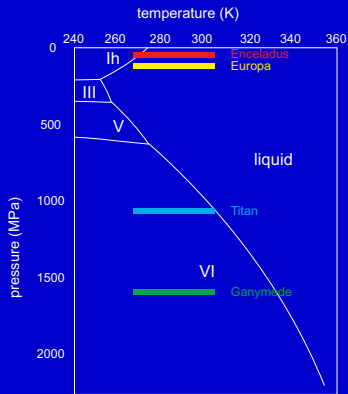
- ▶ a direct contact with silicate core for Enceladus and Europa,



Water phase diagram

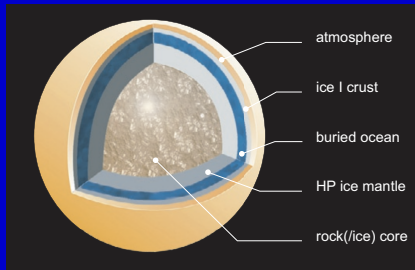
depth of water/rock contact:

moon	$R_s - R_{w/r}$ (km)	g (m/s ²)	$P_{w/r}$ (MPa)
Enceladus	50	0.11	10
Europa	100	1.31	130
Titan	550	1.35	1100
Ganymede	800	1.43	1600

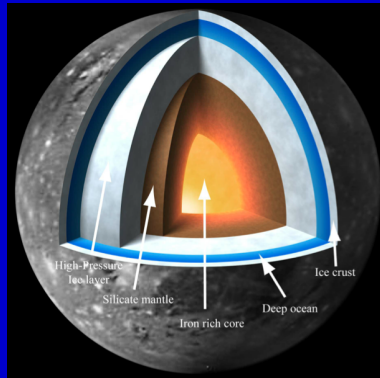


if ocean present beneath an icy crust, isentropic temperature profiles within ocean imply

- ▶ a solid HP ice (V or VI)/silicate core contact for Titan/Ganymede (not always distinguished in this presentation).



An ocean sandwiched between ice Ih and HP ices

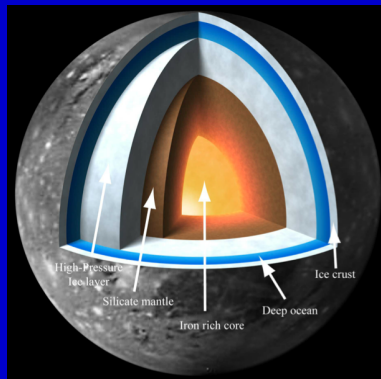


- ▶ **broad questions on such habitats:**

- ⇒ do such environments provide favorable conditions for deep habitats ?

- ⇒ such questions partly addressed by *JUICE*: scrutinize Ganymede as an emblematic example of this class of bodies.

An ocean sandwiched between ice Ih and HP ices

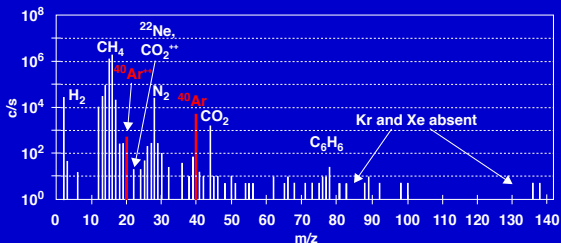


- ▶ more specific questions on dynamics and transport in the HP icy mantle:
 - ⇒ what is the thermal state of the HP icy mantle ?
 - ⇒ what is the vigour of convection in the HP icy mantle ?
 - ⇒ what is the degree of chemical exchanges between the rock core and the ocean through the HP icy mantle ?

Surface evidence for mass/chemical exchanges ?

Titan:

- ▶ detection of radiogenic argon by *Huygens* (Niemann et al., 2010)



⇒ suggests geological activity in the rocky core as well as chemical transport up to the surface,

- ▶ evidence for a salty subsurface ocean from tides, obliquity and electric perturbations (Mitri et al., 2014 ; Baland et al., 2014 ; Beghin et al., 2012).

Ganymede

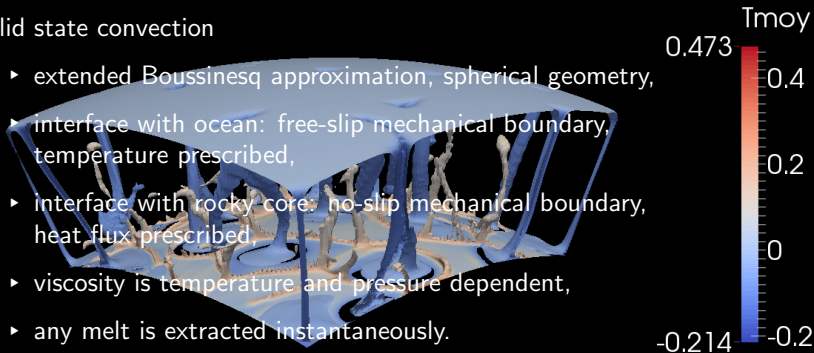
- ▶ evidence for a salty subsurface ocean from small oscillations of auroral ovals (Saur et al., 2015).

Numerical model for HP ice mantle (I)

(3D, simplified melt extraction, large viscosity $\sim 10^{16} - 10^{17}$ Pa s)

solid state convection

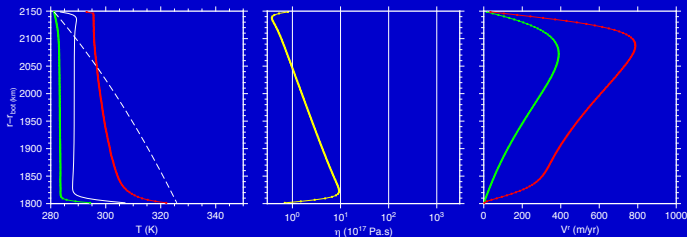
- ▶ extended Boussinesq approximation, spherical geometry,
- ▶ interface with ocean: free-slip mechanical boundary, temperature prescribed,
- ▶ interface with rocky core: no-slip mechanical boundary, heat flux prescribed,
- ▶ viscosity is temperature and pressure dependent,
- ▶ any melt is extracted instantaneously.



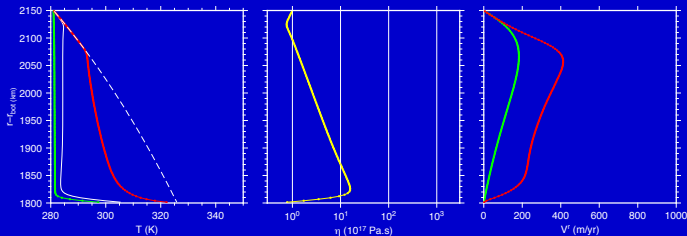
Choblet et al., *Icarus* (2017)

Effect of melting

melt not taken into account (case 1, Durham activation volume)



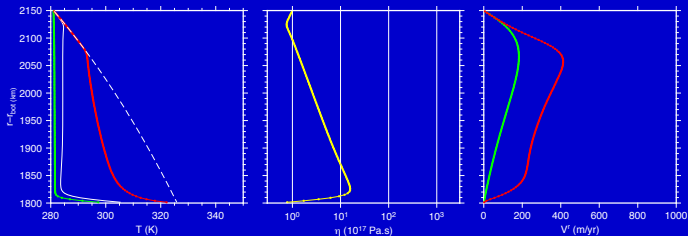
melt extracted (case 1, Durham activation volume)



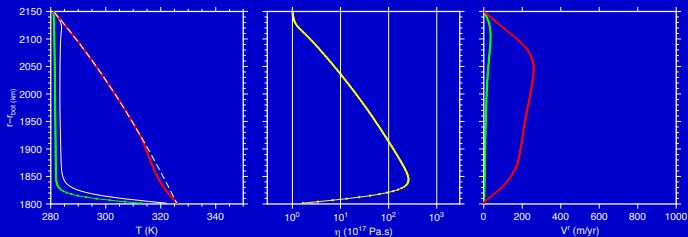
\Rightarrow a slightly smaller (~ 5 K) temperature, velocities are reduced.

Effect of viscosity

case 1, Durham activation volume



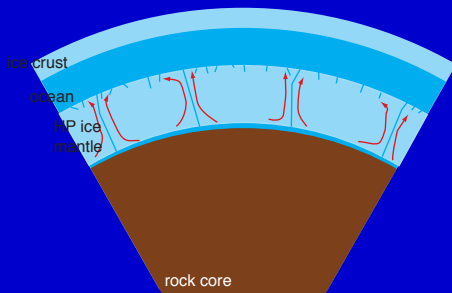
case 1, homologous temperature

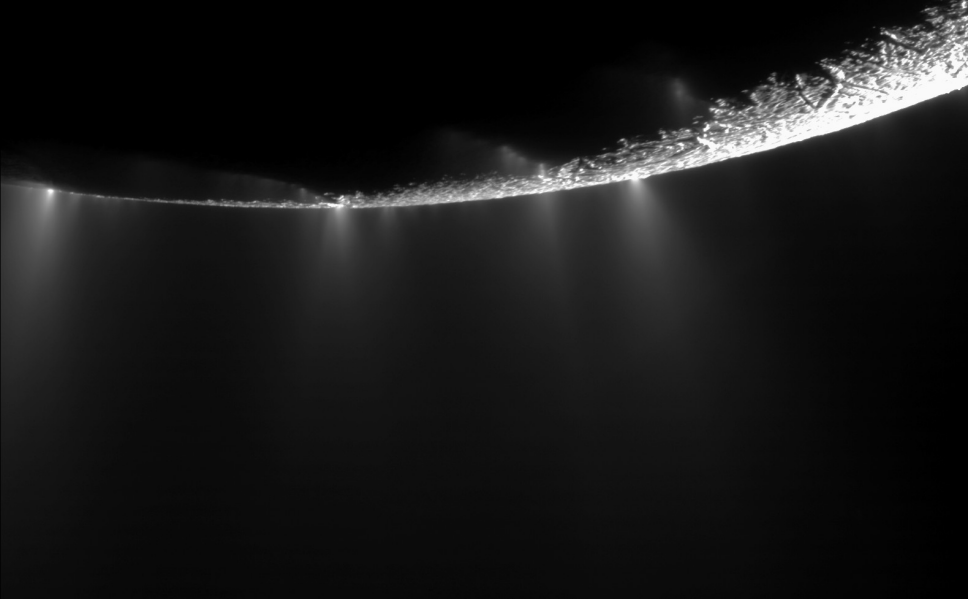


⇒ viscosity increase much more pronounced, maximal temperature much closer to melting curve.

Results: summary

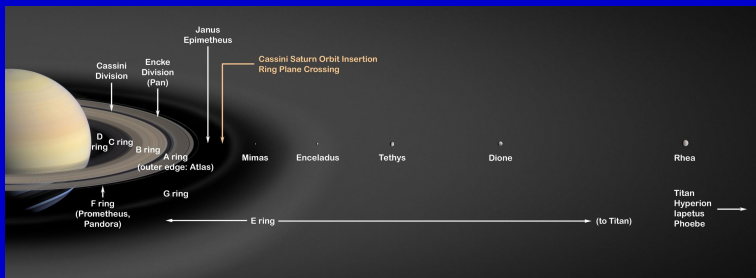
- ▶ power from silicate core mainly transported by melt extraction,
- ▶ average temperature always cool (~ 5 K above surface temperature), mostly depends on layer thickness,
- ▶ melt occurs at HP mantle interface with rocky core,
- ▶ however, maximal temperature at all depths close to melting temperature, often leading to interconnection of melt path, unless HP mantle very thick or viscosity very low





Convection in Enceladus porous core

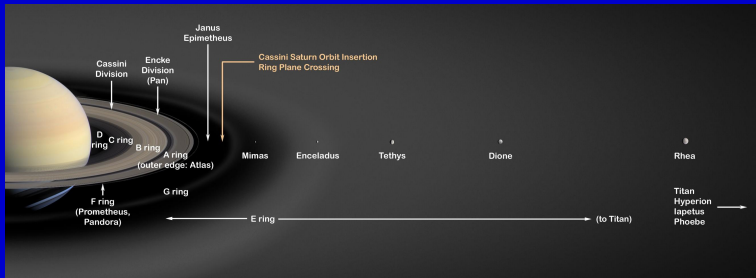
Enceladus in the Saturn system



- ▶ Saturn's (?) sixth moon, $R_s = 252 \text{ km}$, $T \simeq 33 \text{ h}$, $e \simeq 5 \times 10^{-3}$
- ▶ embedded in the densest part of Saturn's diffuse E-ring,
- ▶ *Voyager 2*: contrast between relatively young regions near equator and older, high latitude regions, very much unlike Mimas' ancient cratered surface,

⇒ is Enceladus the source of E-ring's material ? (Terrile and Cook, 1981)

Enceladus in the Saturn system

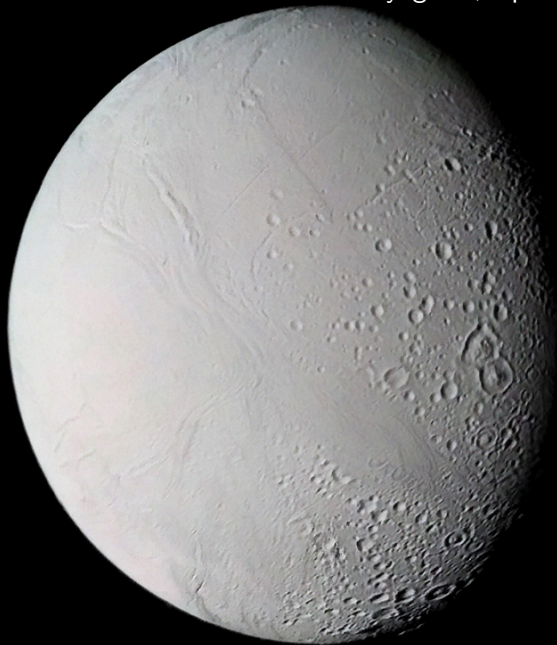


- ▶ Saturn's (?) sixth moon, $R_s = 252 \text{ km}$, $T \simeq 33 \text{ h}$, $e \simeq 5 \times 10^{-3}$
- ▶ embedded in the densest part of Saturn's diffuse E-ring,
- ▶ *Voyager 2*: contrast between relatively young regions near equator and older, high latitude regions, very much unlike Mimas' ancient cratered surface,

⇒ is Enceladus the source of E-ring's material ? (Terrile and Cook, 1981)

yes

Voyager 2, April 26, 1981



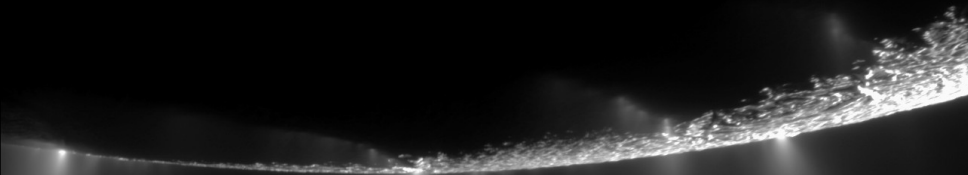
Cassini, January 16, 2005



Cassini, Jan. 7, 2013



Cassini, Feb. 2, 2010



Cassini, July 14, 2005

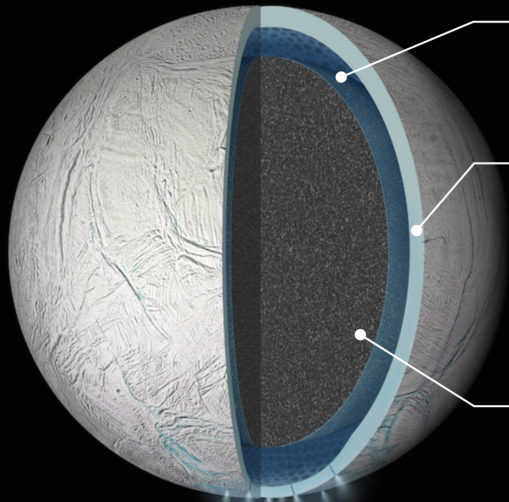
80 79 80 81 91 87 78 74 78 74



What mechanisms power this intense activity ?



Enceladus' interior at the end of Cassini: structure



buried global ocean

30-40 km thick
(Thomas et al., 2016)

very uneven ice shell

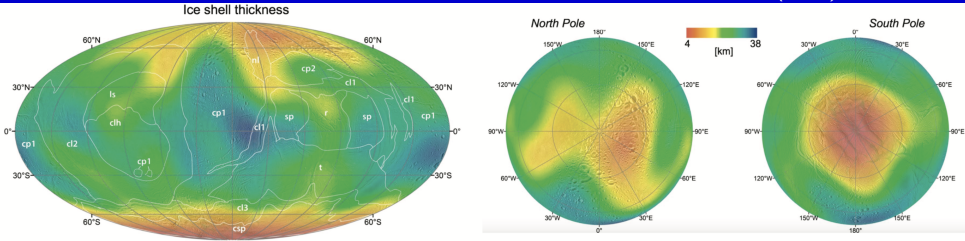
25-30 km thick in average
up to 35 km at equator
less than 5 km at south pole
(Čadek et al., 2016 ;
Beuthe et al., 2016)

porous rock core

filled with 20-30 % water
(e.g. Roberts, 2015 ;
Waite et al., 2017)

Revisiting the heat budget

Čadek et al. (2016)



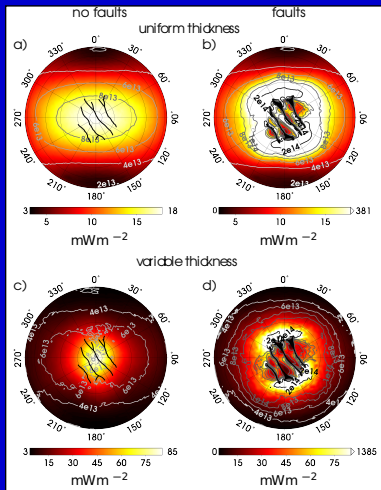
Diffusive equilibrium in a thin ice shell

- ▶ South Polar Terrain (SPT): heat flux $\geq 100\text{-}150 \text{ mW m}^{-2}$ or a total power of 3-5 GW
- ▶ heat flux at low latitudes: $\sim 20\text{-}40 \text{ mW m}^{-2}$
- ▶ global heat loss outside the SPT: $\sim 20\text{-}25 \text{ GW}$

⇒ Total power lost by diffusion $\sim 23\text{-}30 \text{ GW}$
What/where are the heat sources ?

Tidal dissipation within an ice shell of varying thickness

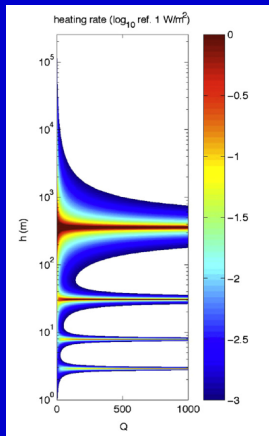
- ▶ thinning at the South Pole strongly enhances tidal dissipation by viscous friction,
- ▶ optimal heat production obtained for ice shell thickness ranging between 1 and 3.5 km for ice viscosity between 10^{14} and 10^{13} Pa s,
- ▶ tidal friction further enhanced by the presence of faults,



Běhounková et al. (2017)

⇒ Dissipation large enough to counterbalance heat loss in the SPT, but not at moderate/northern latitudes.

Tidal heat production in Enceladus' deep interior (1): the ocean

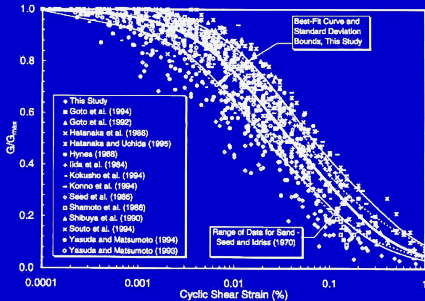


Tyler (2010)

- ▶ dissipation of resonant waves as a response of the subsurface ocean to both eccentricity and obliquity components of tidal forcing (Tyler, 2010 ; Matsuyama et al., 2018),
 - ▶ significant heating obtained for very thin ocean and “inconsistent” pattern (Matsuyama et al., 2018),
- ⇒ overall, unlikely to generate 20-25 GW in the present geometry...

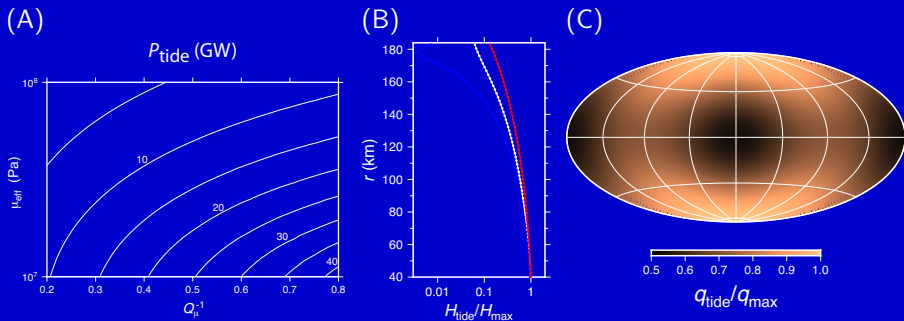
Dissipation of a water saturated mixture of sand/gravel

Rollins et al. (1998)



- ▶ possible mechanisms: inter-granular friction during grain rearrangements or/and frictional sliding along microcracks,
- ▶ anelastic properties of such materials classically parameterized with effective shear modulus and the damping ratio (or dissipation function),
- ▶ a strong decrease in elastic modulus (and increase in dissipation function) is expected when cyclic strain exceeds $\sim 0.01\%$ (typical value for Enceladus tidal deformation in the core, see after),
- ▶ laboratory mechanical tests performed however at larger frequency and lower pressure than those prevailing in Enceladus' core: we expect enhanced dissipation at the very low tidal frequency (creep effects) and a moderate effect of pressure.

Tidal dissipation in Enceladus porous core



⇒ several 10s of GW can be produced with a slightly heterogeneous diffuse pattern: heating is maximal and homogeneous near the centre and decreases more slowly at the poles towards the surface

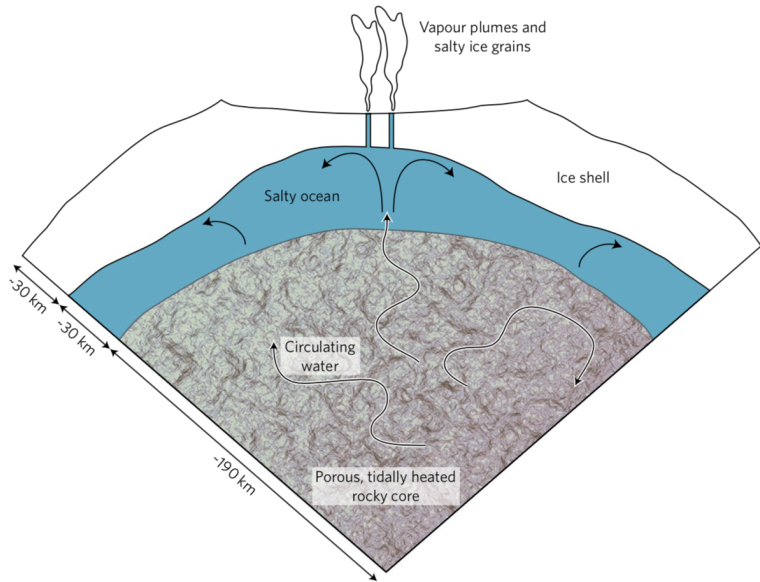


Fig. 1 | Sketch of the interior of Enceladus. Choblet et al. propose a tidally heated core driving hydrothermal circulation⁶. The background internal structure is based on the model presented in ref. ¹³.

Thermal convection of interstitial water in a porous core

Conservation of mass:

$$\nabla \cdot \mathbf{V} = 0 \quad (1)$$

Darcy equation:

$$\mathbf{V} = -\frac{K}{\eta_w \phi} \left(\nabla p_w + \frac{4\pi}{3} \rho_b \rho_w Gr \mathbf{e}^r \right) \quad (2)$$

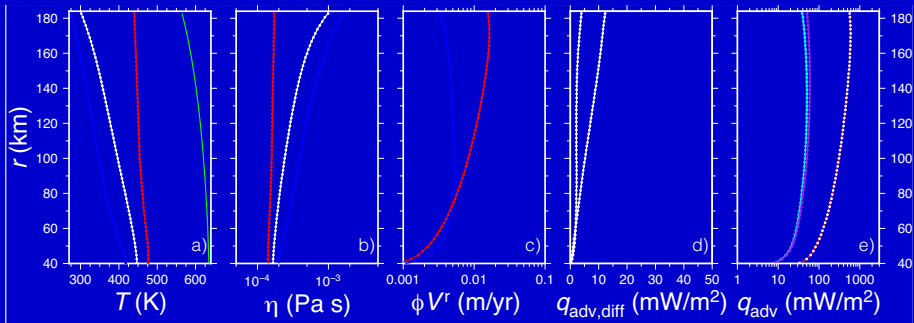
Conservation of energy:

$$C_b \frac{\partial T}{\partial t} + \phi \rho_w c_w \mathbf{V} \cdot \nabla T = k_b \nabla^2 T + H_{\text{tide}} \quad (3)$$

Eqs (1) and (Eq. 2) can be combined to produce a pressure equation solved in our approach:

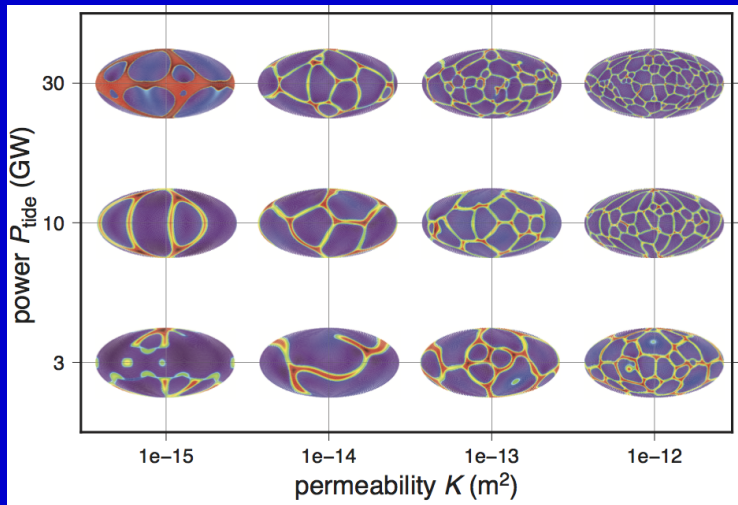
$$\nabla \cdot \left(\frac{1}{\eta_w} (\nabla p_w) \right) = -\gamma \nabla \cdot \left(\frac{\rho_w}{\eta_w} r \mathbf{e}^r \right) \quad (4)$$

Porous convection with homogeneous heating



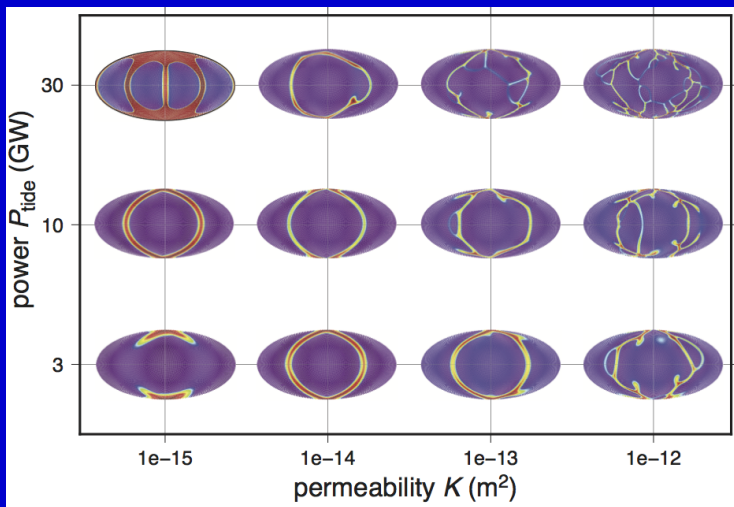
⇒ gradual heating of passive downwellings and buoyant rising in hot narrow upwellings)

Porous convection with homogeneous heating



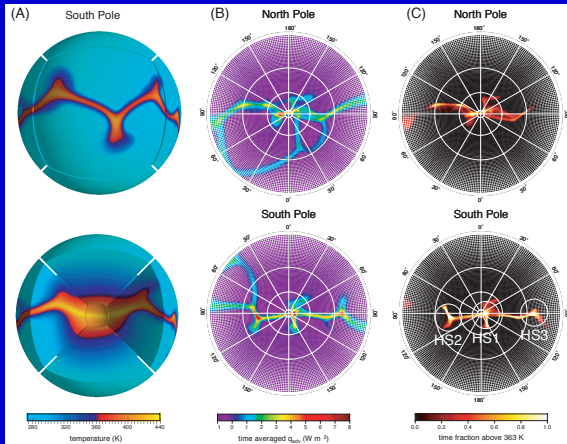
⇒ heat released by narrow, sheet-like upwellings of hot water ($>100^\circ\text{C}$)

Porous convection with heterogeneous (tidal) heating



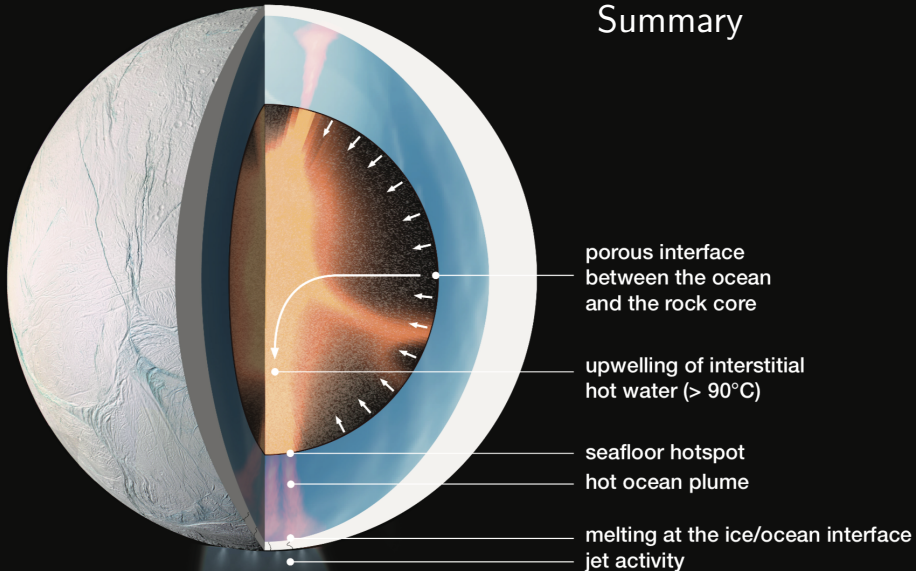
⇒ upwellings concentrated at the poles and trailing/leading meridians where maximal dissipation occurs.

Hot spots at the seafloor



⇒ persistent hotspots (1-5 GW) are anchored beneath the poles.

Summary

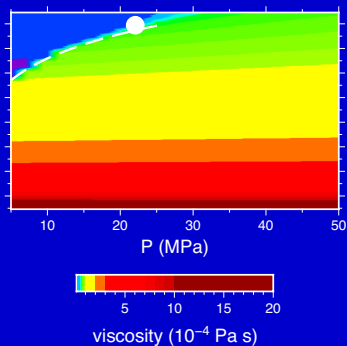
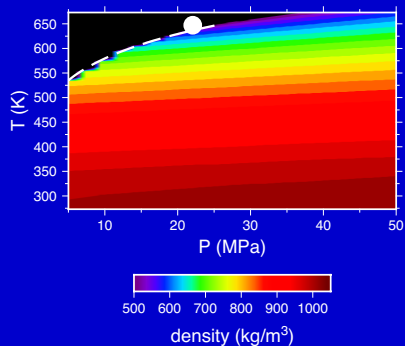


Cassini, Sept. 15, 2006



Porous convection of liquid water in the unconsolidated core

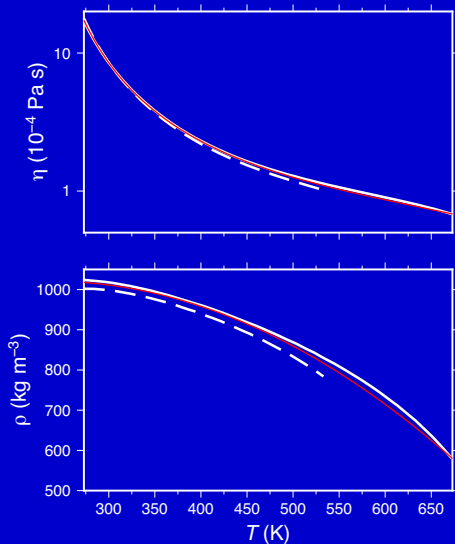
Water properties: density, viscosity



Porous convection of liquid water in the unconsolidated core

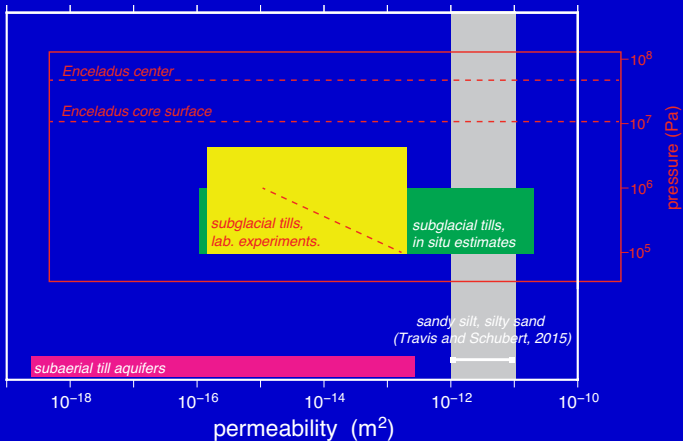
Water properties: density, viscosity

- ▶ effect of pressure (in the range [10, 40] MPa) is neglected
- ▶ critical point never reached in Enceladus' core
- ▶ boiling might occur (not treated consistently in our models)



Porous convection of liquid water in the unconsolidated core

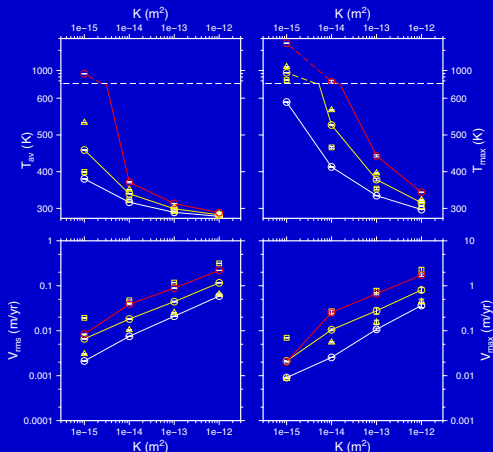
Permeability is the key (yet unknown) variable for porous flow convection



Synthesis of results

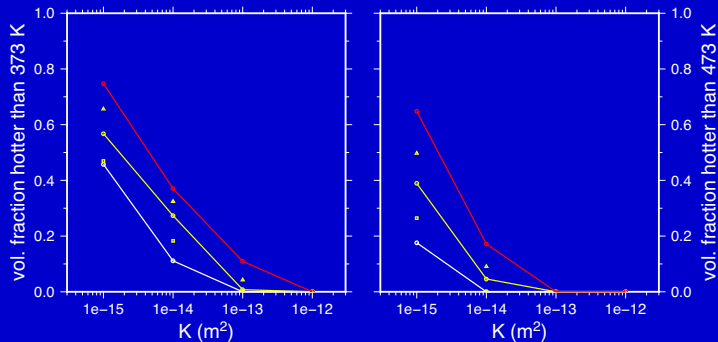
a trade off is observed
between water temperature
and velocity:

- ▶ low K : high T , lower V ,
- ▶ high K : low T , higher V ,



⇒ while the range of admissible values for permeability K is extremely large ($[10^{-18}, 10^{-11}] m^2$, cf. terrestrial analogues), only a limited interval ($[10^{-14}, 10^{-13}] m^2$) is consistent with findings on hydrothermal activity (cf. Hsu et al., 2015)...

Synthesis of results



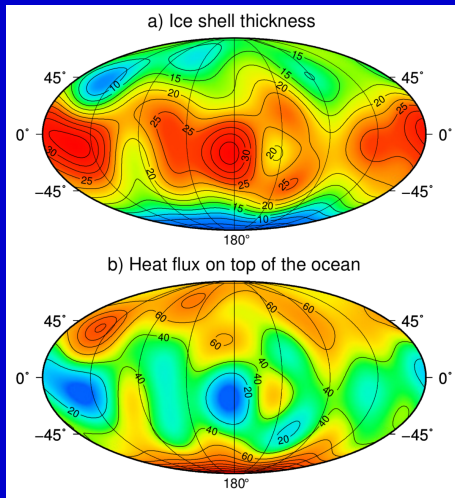
⇒ a significant volume fraction is above $>100^\circ\text{C}$ implying efficient aqueous alteration

The very uneven ice shell as a witness

- ▶ refined analysis (based on shape up to degree $\ell=18$, Tajeddine et al., 2017) confirms earlier results for ice shell structure:

- minimum thickness under polar regions (esp. at the South)
- ice shell thinner along leading/trailing meridians at lower latitudes,

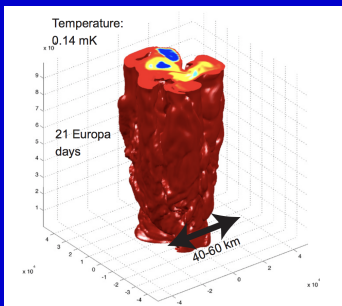
- ▶ predicted heat flux variations resemble the pattern emitted at the sea floor,



Polar ocean plumes: scaling results

	Goodman et al (2004) (scaling and laboratory experiments)	Goodman and Lenferink (2012) (numerical experiments)
l_{cone}/H	0.15	0.2
$V_p/(Hf')$	0.01	$3 \cdot 10^{-3}$
$(\Delta T_p g_o \alpha_o)/(Hf'^2)$	$3 \cdot 10^{-4}$	$4 \cdot 10^{-5}$
l_{cone} (km)	8.25	11
V_p (cm/s)	6	2
ΔT_p (mK)	5	0.7

Table: Characteristics of the oceanic thermal vents.



- ▶ temperature variations within the ocean of a few mK,
- ▶ estimated transport time from seafloor to the source of jets beneath SPT ice shell: a few weeks to months,
- ▶ compatible with the growth rate of nano-silica (*Hsu et al., 2015*)

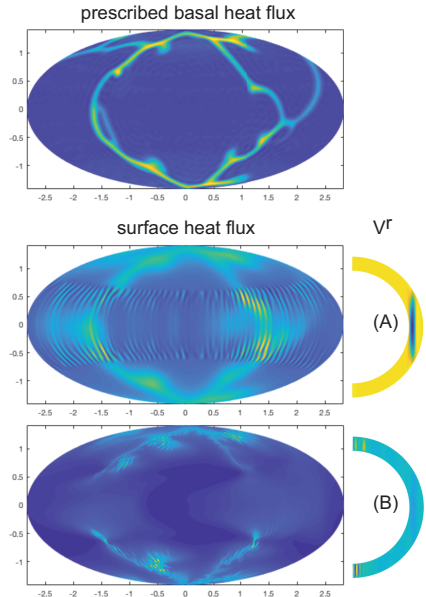
From the seafloor to the ice/ocean interface: dedicated simulations

- ▶ at moderate latitudes bounded by the tangent cylinder, the signal may be blurred depending on the competition between rotation and buoyancy

(A): Coriolis forces are dominant
⇒ thermal convection largely remains outside the tangent cylinder and is visible at the surface of the ocean

(B): Archimedes forces are dominant
⇒ lesser effect of the tangent cylinder, convective instabilities deflected to higher latitudes

- ▶ in polar regions, ocean plumes always imprint the seafloor pattern at the ice/ocean interface.



Solid-state flow of planetary constituents

- ▶ constitutive materials for planets:
metals, rocks (silicates), water,
- ▶ the solid phase is known to possibly flow (creep).



ice: glacier flow observed in the Alps already in 17th century.

Solid-state flow of planetary constituents

- ▶ constitutive materials for planets:
metals, rocks (silicates), water,
- ▶ the solid phase is known to possibly flow (creep).



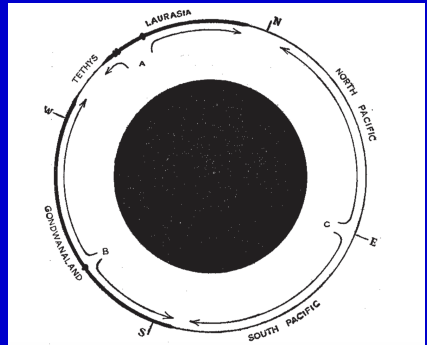
rock: slow rise of Scandinavia above sea-level already observed by Anders Celsius (around 1730, associated to evaporation), the concept of post-glacial rebound appeared later on.

Mantle convection and continental drift

- ▶ once mantle viscosity exhibited from post-glacial rebound, mantle flow on geological time-scales is a possibility,
- ▶ Holmes (1931): connects solid-state mantle convection to continental drift,
- ▶ besides minor errors, modern understanding of mantle convection is proposed.

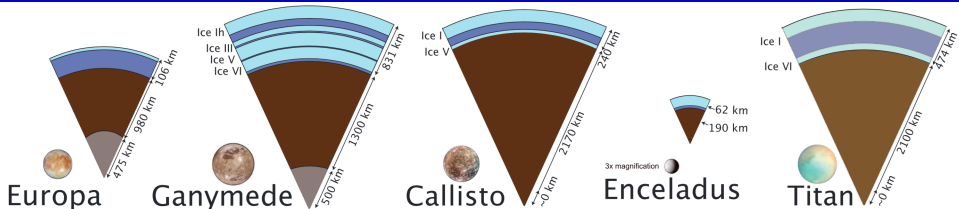
No. XVIII.—RADIOACTIVITY AND EARTH MOVEMENTS. By ARTHUR HOLMES, PROFESSOR OF GEOLOGY, THE UNIVERSITY, DURHAM.

	PAGE.
I. TECTONIC HYPOTHESES	559
II. THE NATURE OF THE CRUST AND SUBSTRATUM	566
III. RADIO-THERMAL ENERGY IN THE ROCKS	570
IV. THE DECREASE OF RADIOACTIVITY WITH DEPTH	572
V. CONVECTION CURRENTS IN THE SUBSTRATUM	575
The Conditions for Convective Circulation	575
The Planetary Circulation	577
The Sub-Continental Circulation	578
VI. SOME GEOLOGICAL CONSEQUENCES	584
Continental Drift	584
Peripheral Mountain Systems	588
Geosynclines	590
Median Areas	593
Rift Valleys	595
Changes of Level of Land and Sea	598
VII. CONCLUSION	600



Holmes (1931)

Big vs. small, diversity: the seafloor



rock/hydrosphere interface:

- ▶ on large moons (Titan, Ganymede) the HP ice mantle is expected to constitute a barrier to chemical interactions between rocks and the ocean,
- ▶ conversely, on smaller moons (Enceladus, Europa) hydrothermal activity might provide a very promising mean for chemical interactions.

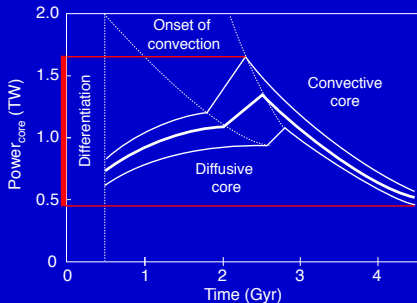
Big vs. small, resemblance: the ice ceiling

ocean/ice interface:

- ▶ while the seafloor has a different nature for the two classes (a phase boundary for large moons vs. a major compositional dichotomy for small moons), lateral gradients in heat flow (and possibly mass flux) could provide a forcing to ocean dynamics ,
- ▶ ocean/atmosphere interaction not obvious:
 - ⇒ stagnant lid regime inherent to convection with strongly temperature-dependent viscosity has to be broken,
 - ⇒ presence of liquid water in a partially molten ice crust might be episodic owing to an intrinsically larger density. . .

Heat power out of the rocky core

thermal history of Titan's rocky core (*Tobie et al., 2006*):



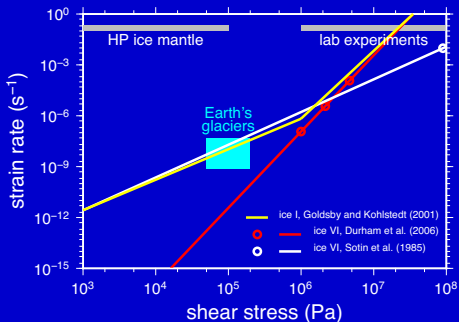
- ▶ three mineralogical compositions and densities reflecting different hydration states,
- ▶ initial conductive stage followed by convective cooling (onset of convection \sim 1.5-2.5 Gyr ago).

\Rightarrow minimal power corresponding to the present-day \sim 0.5 TW,

\Rightarrow maximal power corresponding to the onset of convection $>$ 1.5 TW.

Viscosity of the HP ice

rheology of ice VI measured (*Sotin et al., 1985 ; Durham et al., 1996*) although in limited conditions:

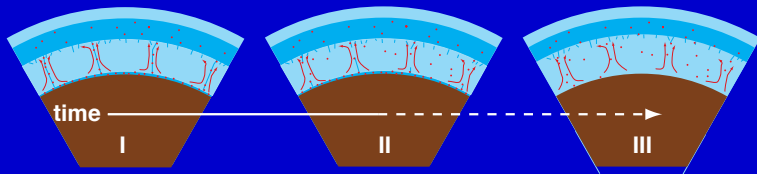


- ▶ considerably higher uncertainties than for ice Ih,
- ▶ apparently, dislocation creep $n > 1$ prevails, although GSS creep is a possibility,
- ▶ probably upper bounds on strength of planetary ice.
- ▶ activation volume not measured for $T > 250K$

⇒ two end-member models for activation volume: either **the estimate of *Durham et al., 1996*** (based on lower T , larger $\dot{\epsilon}$ experiments) or based on **the "homologous" temperature formalism**,

⇒ reasonable viscosity range near the melting point: $\sim 10^{14} - 10^{17} \text{ Pa s}$ (low value corresponding to plausible change in creep mechanism at low stress).

Conclusions



⇒ time evolution and cooling of the moons probably involves successive regimes for melt path,

⇒ due to alleged thinner hydrosphere, Titan more likely than Ganymede to have preserved melt connexion from rocky core to ocean, up to present day (or recent past),

⇒ ultimately, only a full description of heat transfer through HP ices/deep ocean/ice Ih will allow to derive thermal history tailored for each moon.